

AD-A067 991

CORNELL UNIV ITHACA N Y DEPT OF MATERIALS SCIENCE A--ETC F/6 11/6
LOAD RELAXATION STUDIES OF A METALLIC GLASS. (U)
SEP 77 T D HADNAGY, D J KRENITSKY, D G AST

N00014-77-C-0546

UNCLASSIFIED

TR-1

NL

| OF |

AD
A067991



AD A067991

DDC FILE COPY

LEVEL II

B.S. 12

LOAD RELAXATION STUDIES OF A METALLIC GLASS

T.D. Hadnagy, D.J. Krenitsky, D.G. Ast, Che-Yu Li

Contract Number: NR039-151M00014-77-C-0546 *New*

Technical Report #1

September 1977

DDC
RECEIVED
MAY 1 1979
D

79 04 26 048

DISTRIBUTION STATEMENT

Approved for public release,
Distribution Unlimited

UNCLASSIFIED

SECURITY CLASSIFICATION OF THIS PAGE (When Data Entered)

REPORT DOCUMENTATION PAGE		READ INSTRUCTIONS BEFORE COMPLETING FORM
1. REPORT NUMBER Technical Report No. 1	2. GOVT ACCESSION NO	3. RECIPIENT'S CATALOG NUMBER
4. TITLE (and Subtitle) (6) Load Relaxation Studies of a Metallic Glass	(9)	5. TYPE OF REPORT & PERIOD COVERED Technical Progress Report
7. AUTHOR(s) (10) T.D./Hadnagy, D.I./Krenitsky, D.G. Ast, Che-Yu/Li		6. PERFORMING ORG. REPORT NUMBER
9. PERFORMING ORGANIZATION NAME AND ADDRESS Material Science & Eng.; Bard Hall Cornell University, Ithaca, NY 14853	(15)	8. CONTRACT OR GRANT NUMBER(s) (14) TR-1
11. CONTROLLING OFFICE NAME AND ADDRESS Metallurgy Branch Office of Naval Research Arlington, VA 22217	(11)	10. PROGRAM ELEMENT, PROJECT, TASK AREA & WORK UNIT NUMBERS N00014-77-C-0546 New NRO39-151
14. MONITORING AGENCY NAME & ADDRESS (if different from Controlling Office) (12) 17p.		12. REPORT DATE Sep 77
		13. NUMBER OF PAGES 12
		15. SECURITY CLASS. (of this report) Unclassified
		15a. DECLASSIFICATION/DOWNGRADING SCHEDULE
16. DISTRIBUTION STATEMENT (of this Report) Distribution of this document is unlimited		
17. DISTRIBUTION STATEMENT (of the abstract entered in Block 20, if different from Report)		
18. SUPPLEMENTARY NOTES		
19. KEY WORDS (Continue on reverse side if necessary and identify by block number) Metallic Glass, Stress relaxation		
20. ABSTRACT (Continue on reverse side if necessary and identify by block number) The stress relaxation of the Fe-Ni based metallic glass $Fe_{40}Ni_{40}P_{14}B_6$ was investigated in load relaxation experiments. The relaxation consists of a history dependent transient part which is followed by a history independent part where $\epsilon \propto \sigma^4$. The results are analyzed with the equation of state proposed by Hart.		

ACCESSION NO	
015	WITH SECTION
016	EXT. NUMBER
UNCLASSIFIED	
IDENTIFICATION	
BY DISTRIBUTION STATEMENT NUMBER	
017	ANAL. AND IN SPECIAL
A	

DD FORM 1 JAN 73 1473

EDITION OF 1 NOV 65 IS OBSOLETE
S/N 0102-LF-014-6601

Unclassified
SECURITY CLASSIFICATION OF THIS PAGE (When Data Entered)

79 04 26 048

403 152

mt

LOAD RELAXATION STUDIES OF A METALLIC GLASS

T. D. Hadnagy, D. J. Krenisky, D. G. Ast and Che-Yu Li
Department of Materials Science and Engineering
Cornell University, Ithaca, New York 14853

This note reports experimental results of load relaxation studies of a commercial metallic glass (METGLASTM 2826) as a function of temperature. The data suggests that metallic glasses exhibit deformation behavior with flow laws similar to those governing plastic deformation in crystalline solids. The lack of appreciable work hardening on annealed material and the identification of an anelastic component are also indicated by the experimental observation.

The deformation properties of metallic glasses were reviewed recently by Davis.¹ He discussed the possibility that metallic glasses exhibit deformation properties governed by dislocation mechanisms and show little capacity for work hardening. Recently Murata and co-workers² showed that non-elastic deformation in metallic glasses contains two separate components: a time dependent and recoverable anelastic component and a time dependent and non-recoverable plastic component. They argued, however, based on their observations that metallic glasses can be hardened by straining.

Load relaxation experiments have been extensively used in the investigation of non-elastic properties of crystalline solids in conjunction with the work on the development of a plastic equation of state.^{3,4,5} They have the advantage that they can be used to generate stress-strain rate data covering a wide range of strain rate while avoiding the occurrence of plastic instability in the

specimen.⁵ This is particularly useful in the investigation of metallic glasses.

Load relaxation data of a large variety of crystalline solids have shown that the same flow laws for plastic deformation (stress-strain rate relations) apply.^{5,6,7} The contribution of the anelastic deformation component can be identified by the failure of a portion of the stress-strain rate data to be described by the flow laws for plastic deformation.⁵

Based on the work mentioned above a deformation model was developed for non-elastic deformation by using the state variable approach.⁸ In the present work the same model will be adopted to analyze the load relaxation data of metallic glasses.

EXPERIMENTS

The tensile specimen used was made from a commercial metallic glass ribbon [METGLASTM 2826 (0.65x0.0023 in.)] by polishing with 220 grit emery-paper. It had a gage section of 2.2x0.006x0.15 cm. The load relaxation experiment was carried out by using a table model Instron testing system. After the temperature of the specimen and the testing system was stabilized, the specimen was loaded at an extension rate of .02 in/min (.056 cm/sec) to the desired stress level. The crosshead was then fixed and load relaxation resulted from the conversion of the combined elastic strain of the test system and the specimen to non-elastic strain of the specimen. The rate of load relaxation was related to the non-elastic strain rate of the specimen through the combined modulus of the test system and specimen. The experiment yielded data in the form of load vs. time which was analyzed to yield a $\log \sigma$ vs $\log \dot{\epsilon}$ (σ , stress and $\dot{\epsilon}$, non-elastic strain rate) curve for a particular load relaxation run. Throughout this study the specimen deformed homogeneously without the formation of shear band.

RESULTS AND DISCUSSION

Typical load relaxation data obtained at 270°C in the form of $\log \sigma - \log \dot{\epsilon}$ curves are shown in Figure 1. Each curve represents the data obtained from a load relaxation run. The specimen used was first annealed at 300° for 8 hours prior to the load relaxation experiment at 270°C. All the curves shown in Figure 1 were obtained on a single specimen, by re-loading the specimen after a load relaxation run to a higher stress level and continuing raising the stress of each subsequent run until failure. The length of each

load relaxation run ranged from a few hours to in excess of a day. The order of the runs are as given in Figure 1. The data of the first run and the third run are not shown due to alignment and temperature control problem respectively.

Each $\log \sigma - \log \dot{\epsilon}$ curve suggests distinctly two types of behavior. The initial portion of the load relaxation data (high strain rate portion) shows an extremely high stress exponent (>100 , the inverse of the slope of the $\log \sigma - \log \dot{\epsilon}$ curve). As the experiment proceeds (low strain rate portion), all the $\log \sigma - \log \dot{\epsilon}$ data merge into a single curve and show a significantly lower stress exponent of about 4. These results are consistent with the deformation model based on the state variable approach and the experience gained on crystalline solids^{3,4,5,6} such that the initial high strain rate portion of the relaxation data reflect the contribution of anelastic deformation and the low strain rate portion of the data show the stress-strain rate relation of plastic deformation. These results also suggest the lack of significant work hardening as well as the absence thermally induced structural change. Discussion will be made in the following to support these possibilities.

The deformation model of interest was developed to describe the non-elastic properties of the grain matrix of crystalline solids and has been tested extensively by using a variety of crystalline metals and alloys.^{3,4,5,8} It consists of two branches in parallel. One of the branches includes an anelastic spring in series with a plastic element ($\dot{\epsilon}$ -element) which governs plastic deformation at high homologous temperatures and/or low strain rates. The other branch contains a non-elastic friction element which

represents dislocation glide controlled processes and is important at low homologous temperatures and/or high strain rates. The magnitude of the anelastic strain α is linearly related to the stress on the anelastic spring through its modulus. The non-elastic strain rate of the specimen $\dot{\epsilon}$ is represented by

$$\dot{\epsilon} = \dot{\alpha} + \dot{\alpha} \quad (1)$$

where $\dot{\alpha}$ is the anelastic strain rate and $\dot{\alpha}$ is the plastic strain rate of the $\dot{\alpha}$ -element. The following relations are of present interest:

$$\ln(\sigma^*/\sigma_a) = (\dot{\epsilon}^*/\dot{\alpha})^\lambda \quad (2)$$

$$\dot{\epsilon} = \dot{\alpha}^*(\sigma_f/M)^M \quad (3)$$

$$\sigma = \sigma_a + \sigma_f \quad (4)$$

$$\sigma_a = M\alpha \quad (5)$$

where σ^* is the hardness parameter which measures the hardness state of the specimen, σ_a is the stress on the $\dot{\alpha}$ -element, σ_f is the stress on the element controlled by dislocation glide, $\dot{\epsilon}^*$ is the rate constant for the $\dot{\alpha}$ -element, $\dot{\alpha}^*$ is the rate constant for dislocation glide controlled element, σ is applied stress, M is the anelastic modulus and λ and M are two constants which determine the shape of the constant hardness (σ^*) $\log \sigma - \log \dot{\epsilon}$ curve.

The hardness parameter σ^* determines a unique $\log \sigma - \log \dot{\epsilon}$ curve and can be changed by work hardening or by thermally induced structural changes. Equations (2) and (3) above represents the $\dot{\alpha}$ -element and the dislocation glide controlled element respectively. Typical values of λ and M for crystalline metals and alloys are λ , near 0.15 and M , between 7.5-8.^{3,4,8}

According to the above model, during the initial loading of

the specimen, the non-elastic strain rate of the specimen reflects mostly the inelastic strain rate $\dot{\epsilon}$. This is because the initially stored anelastic strain of a well annealed specimen is close to zero. As the crosshead is fixed, the initial portion of the load relaxation is still controlled by the anelastic strain rate $\dot{\epsilon}$ due to the fact that the build-up of stored anelastic strain is governed by Equation (3) and requires a finite time. Consequently the initial portion of the $\log \sigma - \log \dot{\epsilon}$ data cannot be presented by either Equation (2) or (3). At longer relaxation times, the rate of load relaxation decreases and plastic deformation becomes important. For the interest of the present discussion, the shape of the low strain rate portion of the $\log \dot{\sigma} - \log \dot{\epsilon}$ curve [Equation (2)] reflects the extremely high hardness (σ^*) value involved. During the later stages of the relaxation period the stored anelastic strain will decrease significantly with time as described by Equations (3) and (5). Thus during reloading and the portion of the load relaxation immediately following reloading the anelastic strain rate $\dot{\epsilon}$ will be controlling again.

If following reloading to a higher stress the specimen has not been hardened by deformation (σ^* unchanged), the $\log \sigma - \log \dot{\epsilon}$ data obtained after anelasticity has taken its toll, will coincide with those obtained in the previous load relaxation run within the error of the experiment. This is shown by the data in Figure 1. A more detailed analysis shows very small but systematic shifts of the order of the experimental error of the slope of these curves. It is noted that for crystalline solids, after reloading to a higher stress level, because of work hardening, invariably a substantially new $\log \sigma - \log \dot{\epsilon}$ curve will result. It is noted also the data shown in Figure 2 suggests the absence of a thermally in-

duced structural change.

The existence of both the anelastic component and the plastic component of deformation suggested above and the very low stress dependence for plastic flow reflected by the overlapping portion of the $\log \sigma - \log \dot{\epsilon}$ curves in Figure 1 are consistent with the results reported by Murata et al. The low strain rate portion of the data can be represented by Equation (2) which describes the plastic properties of a variety of crystalline metals and alloys.^{3,4,5,6} The solid curve in Figure 1 is calculated by using Equation (2) with a value of $\log \sigma^* = 5.9$ (σ^* in psi) and $\log \dot{\epsilon}^* = -5.6$.

The low stress dependence for plastic flow shown by the present data is a direct consequence of the high σ^* involved according to the deformation model.⁵ The value of σ^* can be used to estimate the flow stress at high strain rates for crystalline solids.⁵ The value of σ^* (7.9×10^5 psi or 547 MPa) given above is considerably higher than the high flow stresses reported in the literature for Fe-Ni base metallic glasses.¹ It is possible that the flow stress determination in a tensile test on metallic glasses will be lower than σ^* according to Equation (2). Based on recent work on work-hardening, the ability of a material to work harden is significantly reduced at high hardnesses (σ^*).⁵ The lack of work-hardening suggested by the data in Figure 1 is therefore consistent with the high σ^* value given above. Essentially the present data suggest that we are observing here the properties of a highly work-hardened crystalline solid. The deformation model will predict therefore little capacity for work hardening and a low stress dependence for plastic flow.

Figure 2 shows load relaxation data at 270°C obtained by using a specimen in the as-received condition without annealing at 300°C

prior to the load relaxation experiment. These $\log \sigma - \log \dot{\epsilon}$ curves have shapes similar to those given in Figure 1. However, the low strain rate portion (plastic part) of these curves do not coincide as well as those shown in Figure 1 reflecting the effects of structural rearrangement. Apparently annealing at 300°C improved the stability of the structure of the specimen. The improved stability found just below the annealing temperature has also been shown by Krenitsky and Ast⁹ in their work on shear band deformation.

Figure 3 shows the load relaxation data obtained at room temperature by using as-received specimens. More than one specimen was used to obtain these curves. These curves show extremely high stress exponent (the inverse of the slope of the $\log \sigma - \log \dot{\epsilon}$ curve). By comparing with the curves in Figure 1, the room temperature curve suggests qualitatively the importance of anelastic deformation. Work is in progress in this laboratory to determine the flow laws for anelastic deformation in metallic glasses and to compare with those found in crystalline solids.⁷ It should be noted that the data fit by using Equation (2) and shown in Figure 1 depends on the identification of the high strain rate portion of the $\log \sigma - \log \dot{\epsilon}$ curve to be controlled by anelastic deformation. Information obtained on anelastic deformation together with the constitutive relations given previously can be used to account for the high strain rate portion of the $\log \sigma - \log \dot{\epsilon}$ data quantitatively in order to support the present analysis of the low strain rate portion of load relaxation data.

In summary the load relaxation data obtained in this work suggest the possibility that non-elastic deformation in metallic glasses is controlled by dislocation mechanisms. Both the anelastic component and the plastic component of deformation were identified

and the latter was found to be described by the same flow laws as those for plastic deformation in crystalline solids. The present data also supports the lack of substantial work hardening in metallic glasses.

This work is supported by Energy Research and Development Administration and by the Office of Naval Research.

REFERENCES

1. Lance A. Davis, Paper presented at the 1976 ASM Seminar on Metallic Glasses, Niagara Falls, N.Y., September 18-19. Proceedings to be published by American Society of Metals, 1977.
2. T. Murata, H. Kimura and T. Masanoto, Scripta Met., Vol. 10, p. 705, (1976).
3. F. H. Huang, F. V. Ellis, C.Y. Li, Metallurgical Transactions A, Vol. 8, p. 699 (1977).
4. N. Nir, F. H. Huang, E. W. Hart, C. Y. Li, Metallurgical Transactions A, Vol. 8A, p. 583 (1977).
5. E. W. Hart, Che-Yu Li, H. Yamada, and G. L. Wire: "Phenomenological Theory: A Guide to Constitutive Relations and Fundamental Deformation Properties," in Constitutive Equations in Plasticity, A. Argon, ed., p. 149, MIT Press, (1975).
6. E. W. Hart, Acta. Met., Vol. 18, p. 599 (1970).
7. N. Nir, E. Hart, C. Y. Li, Scripta Metallurgica, Vol. 10, p. 189 (1976).
8. E. W. Hart, J. Eng. Mater. Technol., Vol. 98, p. 193 (1976).
9. D. Krenitsky and D. Ast, to be published.

FIGURE CAPTIONS

Figure 1: Log σ - Log $\dot{\epsilon}$ data for METGLAS 2826 obtained at 270°C after an 8 hr. anneal at 300°C.

Figure 2: Log σ - Log $\dot{\epsilon}$ data for METGLAS 2826 obtained at 270°C without preannealing.

Figure 3: Log σ - Log $\dot{\epsilon}$ data for METGLAS 2826 obtained at 20°C.

1. T. Murata, H. Kimura and T. Masanoto, *Scripta Met.*, 10, 705 (1976).
2. F. H. Huang, F. V. Ellis, C.Y. Li, *Met. Trans. A*, 8, 699 (1977).
3. N. Nir, F. H. Huang, E. W. Hart, C. Y. Li, *Met. Trans. A*, 8A, 583 (1977).
4. E. W. Hart, Che-Yu Li, M. Yamada, and G. L. Wire: "Phenomenological Theory: A Guide to Constitutive Relations and Fundamental Deformation Properties", in *Constitutive Equations in Plasticity*, A. Argon, ed., p. 149, MIT Press (1975).
5. E. W. Hart, *Acta Met.*, 18, 599 (1970).
6. N. Nir, E. Hart, C. Y. Li, *Scripta Met.* 10, 189 (1976).
7. E. W. Hart, *J. Engr. Mater. Technol.*, 98, 193 (1976).
8. D. Krenitsky and D. Ast, to be published.

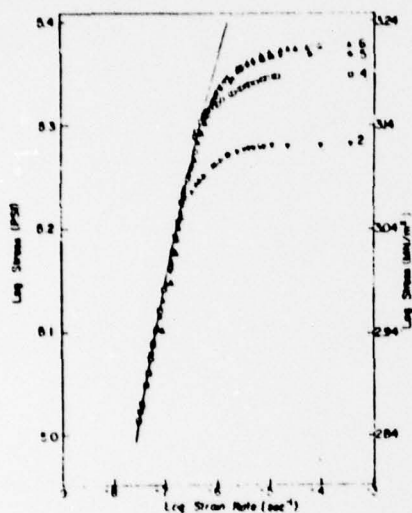


Figure 1

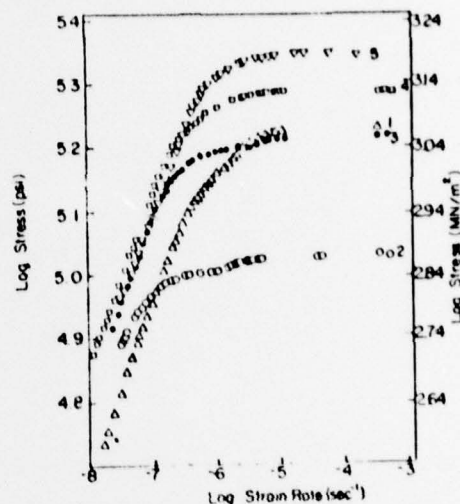


Figure 2

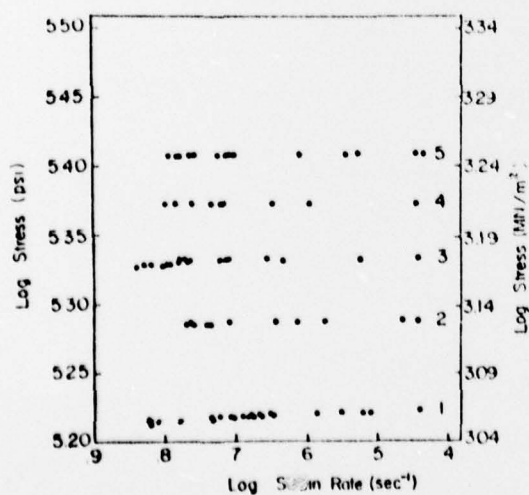


Figure 3

BASIC DISTRIBUTION LIST

Technical and Summary Reports

April 1978

<u>Organization</u>	<u>Copies</u>	<u>Organization</u>	<u>Copies</u>
Defense Documentation Center Cameron Station Alexandria, VA 22314	12	Naval Air Propulsion Test Center Trenton, NJ 08628 ATTN: Library	1
Office of Naval Research Department of the Navy 800 N. Quincy Street Arlington, VA 22217		Naval Construction Battalion Civil Engineering Laboratory Port Hueneme, CA 93043 ATTN: Materials Division	1
ATTN: Code 471	1	Naval Electronics Laboratory	
Code 102	1	San Diego, CA 92152	
Code 470	1	ATTN: Electron Materials Sciences Division	1
Commanding Officer Office of Naval Research Branch Office Building 114, Section D 666 Summer Street Boston, MA 02210	1	Naval Missile Center Materials Consultant Code 3312-1 Point Mugu, CA 92041	1
Commanding Officer Office of Naval Research Branch Office 536 South Clark Street Chicago, IL 60605	1	Commanding Officer Naval Surface Weapons Center White Oak Laboratory Silver Spring, MD 20910 ATTN: Library	1
Office of Naval Research One Hallidie Plaza Suite 601 San Francisco, CA 94102	1	David W. Taylor Naval Ship Research and Development Center Materials Department Annapolis, MD 21402	1
Naval Research Laboratory Washington, DC 20375		Naval Undersea Center San Diego, CA 92132 ATTN: Library	1
ATTN: Codes 6000	1	Naval Underwater System Center	
6100	1	Newport, RI 02840	
6300	1	ATTN: Library	1
6400	1		
2627	1	Naval Weapons Center China Lake, CA 93555 ATTN: Library	1
Naval Air Development Center Code 302 Warminster, PA 18964 ATTN: Mr. F. S. Williams	1	Naval Postgraduate School Monterey, CA 95940 ATTN: Mechanical Engineering Department	1

BASIC DISTRIBUTION LIST (cont'd)

<u>Organization</u>	<u>Copies</u>	<u>Organization</u>	<u>Copies</u>
Naval Air Systems Command Washington, DC 20360 ATTN: Codes 52031 52032	1	NASA Headquarters Washington, DC 20546 ATTN: Code RRM	1
Naval Sea System Command Washington, DC 20362 ATTN: Code 035	1	NASA Lewis Research Center 21000 Brookpark Road Cleveland, OH 44135 ATTN: Library	1
Naval Facilities Engineering Command Alexandria, VA 22331 ATTN: Code 03	1	National Bureau of Standards Washington, DC 20234 ATTN: Metallurgy Division Inorganic Materials Div.	1
Scientific Advisor Commandant of the Marine Corps Washington, DC 20380 ATTN: Code AX	1	Director Applied Physics Laboratory University of Washington 1013 Northeast Forthleith Street Seattle, WA 98105	1
Naval Ship Engineering Center Department of the Navy Washington, DC 20360 ATTN: Code 6101	1	Defense Metals and Ceramics Information Center Battelle Memorial Institute 505 King Avenue Columbus, OH 43201	1
Army Research Office P.O. Box 12211 Triangle Park, NC 27709 ATTN: Metallurgy & Ceramics Program	1	Metals and Ceramics Division Oak Ridge National Laboratory P.O. Box X Oak Ridge, TN 37380	1
Army Materials and Mechanics Research Center Watertown, MA 02172 ATTN: Research Programs Office	1	Los Alamos Scientific Laboratory P.O. Box 1663 Los Alamos, NM 87544 ATTN: Report Librarian	1
Air Force Office of Scientific Research Bldg. 410 Bolling Air Force Base Washington, DC 20332 ATTN: Chemical Science Directorate Electronics & Solid State Sciences Directorate	1	Argonne National Laboratory Metallurgy Division P.O. Box 229 Lemont, IL 60439	1
Air Force Materials Laboratory Wright-Patterson AFB Dayton, OH 45433	1	Brookhaven National Laboratory Technical Information Division Upton, Long Island New York 11973 ATTN: Research Library	1
Library Building 50, Rm 134 Lawrence Radiation Laboratory Berkeley, CA	1	Office of Naval Research Branch Office 1030 East Green Street Pasadena, CA 91106	1

SUPPLEMENTARY DISTRIBUTION LIST

Technical and Summary Reports

November 1978

Professor G. S. Ansell
Rensselaer Polytechnic Institute
Department of Metallurgical
Engineering
Troy, NY 12181

Professor Dieter G. Ast
Cornell University
Department of Materials Science
and Engineering
Ithaca, NY 14853

Dr. E. M. Breinan
United Technologies Corporation
United Technologies Research Center
East Hartford, CT 06103

Professor H. D. Brody
University of Pittsburgh
School of Engineering
Pittsburgh, PA 15213

Dr. R. W. Cahn
University of Sussex
School of Engineering and
Applied Science
Brighton BN1 9QT
ENGLAND

Dr. E. A. Clark
Solid State Division
Naval Surface Weapons Center
White Oak Laboratory
Silver Spring, MD 20910

Dr. S. M. Copley
University of Southern California
Los Angeles, CA 90007

Professor M. Cohen
Massachusetts Institute of Technology
Department of Metallurgy
Cambridge, MA 02139

Dr. R. B. Diegle
Battelle
505 King Avenue
Columbus, OH 43201

Professor B. C. Giessen
Northeastern University
Department of Chemistry
Boston, MA 02115

Professor N. J. Grant
Massachusetts Institute of Technology
Department of Materials Science
and Engineering
Cambridge, MA 02100

Dr. F. E. Luborsky
General Electric Company
P. O. Box 8
Corporate R&D
Schenectady, NY 12301

Dr. J. Perel
Phrasor Technology
1536 Highland Avenue
Duarte, CA 91010

Professor O. D. Sherby
Stanford University
Materials Science Division
Stanford, CA 94300

Professor D. Turnbull
Harvard University
Division of Engineering and
Applied Physics
Cambridge, MA 02138

Professor R. Mehrabian
University of Illinois
Department of Mechanical and
Industrial Engineering
Urbana, IL 61801

Professor P. R. Strutt
University of Connecticut
School of Engineering
Department of Metallurgy
Storrs, CT 06268